Metformin, phenformin, and galegine inhibit complex IV activity and reduce glycerol-derived gluconeogenesis

Traci E. LaMoia[a,b] (iD), Gina M. Butrico[a], Hasini A. Kalpage[c], Leigh Goedeke[a] (iD), Brandon T. Hubbard[a,b], Daniel F. Vatner[a] (iD), Rafael C. Gaspar[a], Xian-Man Zhang[a], Gary W. Cline[a], Keita Nakahara[d], Seungwan Woo[d], Atsuhiro Shimada[d], Maik Hüttemann[c], and Gerald I. Shulman[a,b,1] (iD)

[a]Department of Internal Medicine, Yale School of Medicine, New Haven, CT 06520; [b]Department of Cellular and Molecular Physiology, Yale School of Medicine, New Haven, CT 06520; [c]Center for Molecular Medicine and Genetics, Wayne State University School of Medicine, Detroit, MI 48201; and [d]Department of Applied Life Science, Gifu University, Gifu 501-1193, Japan

Metformin exerts its plasma glucose-lowering therapeutic effect primarily through inhibition of hepatic gluconeogenesis. However, the precise molecular mechanism by which metformin inhibits hepatic gluconeogenesis is still unclear. Although inhibition of mitochondrial complex I is frequently invoked as metformin's primary mechanism of action, the metabolic effects of complex I inhibition have not been thoroughly evaluated in vivo. Here, we show that acute portal infusion of piericidin A, a potent and specific complex I inhibitor, does not reduce hepatic gluconeogenesis in vivo. In contrast, we show that metformin, phenformin, and galegine selectively inhibit hepatic gluconeogenesis from glycerol. Specifically, we show that guanides/biguanides interact with complex IV to reduce its enzymatic activity, leading to indirect inhibition of glycerol-3-phosphate (G3P) dehydrogenase (GPD2), increased cytosolic redox, and reduced glycerol-derived gluconeogenesis. We report that inhibition of complex IV with potassium cyanide replicates the effects of the guanides/biguanides in vitro by selectively reducing glycerol-derived gluconeogenesis via increased cytosolic redox. Finally, we show that complex IV inhibition is sufficient to inhibit G3P-mediated respiration and gluconeogenesis from glycerol. Taken together, we propose a mechanism of metformin action in which complex IV–mediated inhibition of GPD2 reduces glycerol-derived hepatic gluconeogenesis.

gluconeogenesis | complex I | complex IV | biguanides | redox

Metformin (1,1-dimethylbiguanide) is the standard first-line pharmaceutical intervention for type 2 diabetes mellitus (T2D) and is one of the most widely prescribed drugs worldwide (1, 2). Metformin and other more potent synthetic guanide/biguanide derivatives, such as phenformin (*N*-phenethylbiguanide), have glucose-lowering effects in patients with T2D. Following oral administration, metformin accumulates to a high degree within the liver due to first-pass uptake in the portal vein following absorption from the gut, and the presence of the organic cation transporter 1 (OCT1) in the sinusoidal endothelial cells of the liver (3–7). This is in contrast to skeletal and cardiac muscle, where OCT1 is not highly expressed. The observed glucose-lowering effects in individuals with poorly controlled T2D can mostly be attributed to inhibition of hepatic gluconeogenesis, as opposed to altering insulin sensitivity or secretion (8–13); however, despite the extensive literature spanning several decades examining metformin's effects in vivo and in vitro, a consensus on metformin's precise mechanism of action still does not exist.

The most well-studied mechanism is complex I inhibition, which is central to several frequently invoked mechanisms of metformin action, including adenosine monophosphate (AMP)-activated protein kinase activation, decreased energy charge ([adenosine triphosphate {ATP}]:[adenosine diphosphate {ADP}] and [ATP]:[AMP] ratios), and AMP inhibition of fructose 1,6-bisphosphatase, among others (14–18). Yet, complex I inhibition is

only observed at suprapharmacological concentrations (>1 mM) of metformin, which is severalfold higher than concentrations achieved in vivo (3, 7, 19, 20). Furthermore, no study to date has convincingly demonstrated that complex I inhibition can, in fact, replicate metformin's glucose-lowering effects in vivo. To address this question, we sought to specifically inhibit complex I activity in vivo to determine whether the metabolic effects of impaired complex I activity resemble those observed with metformin.

We and others have previously proposed an alternative mechanism of metformin action, in which alterations in hepatic redox state and inhibition of glycerol-3-phosphate dehydrogenase (GPD2) potentiate metformin's glucose-lowering effects (20–22). GPD2 is central to the α-glycerophosphate shuttle, one of two redox shuttles, which transfers reducing equivalents from the cytosol to the mitochondrial matrix. Specifically, GPD2 transfers electrons to mitochondrial ubiquinone, generating ubiquinol that is reoxidized by complex III (ubiquinol cytochrome *c* reductase) of the electron transport chain

Significance

Metformin is the most commonly prescribed drug for the treatment of type 2 diabetes mellitus, yet the mechanism by which it lowers plasma glucose concentrations has remained elusive. Most studies to date have attributed metformin's glucose-lowering effects to inhibition of complex I activity. Contrary to this hypothesis, we show that inhibition of complex I activity in vitro and in vivo does not reduce plasma glucose concentrations or inhibit hepatic gluconeogenesis. We go on to show that metformin, and the related guanides/biguanides, phenformin and galegine, inhibit complex IV activity at clinically relevant concentrations, which, in turn, results in inhibition of glycerol-3-phosphate dehydrogenase activity, increased cytosolic redox, and selective inhibition of glycerol-derived hepatic gluconeogenesis both in vitro and in vivo.

(ETC) (23). Thus, excess mitochondrial ubiquinol decreases GPD2 activity and increases reducing equivalents in the cytosol, which can be experimentally represented by an increased [lactate]:[pyruvate] ratio (referred to here as increased cytosolic redox state). Increased cytosolic redox is predicted to selectively reduce gluconeogenesis from reduced substrates (e.g., lactate and glycerol), while gluconeogenesis from nonreduced substrates (e.g., alanine, dihydroxyacetone phosphate [DHAP], and pyruvate) is unaffected (24), which is in contrast to a complex I-dependent mechanism of metformin action. This is consistent with metformin's effects in both humans and rodents (12, 20, 25).

Clinical studies have shown that the glucose-lowering effects of metformin in patients with fasting hyperglycemia, due to poorly controlled T2D, can mostly be attributed to reductions in hepatic glucose production (HGP); however, these effects are not consistently observed in normoglycemic individuals (8, 26, 27). These paradoxical effects provide insights into potential mechanisms of metformin action in humans: Individuals with poorly controlled T2D have dysregulated white adipose tissue (WAT) lipolysis, leading to increased flux of fatty acids and glycerol delivery to the liver, the latter of which increases hepatic gluconeogenesis through a substrate push mechanism (28–33). Accordingly, selective inhibition of glycerol-derived gluconeogenesis, due to increased cytosolic redox, may explain metformin's paradoxical effects, but this has not yet been demonstrated in vivo.

Here, we examined whether targeted inhibition of complex I using piericidin A, a specific and irreversible inhibitor of mitochondrial nicotinamide adenine dinucleotide reduced (NADH)–ubiquinone oxidoreductase (complex I), is sufficient to mediate metformin's glucose-lowering effects in vitro and in vivo. We also examine the effects of metformin, two more potent guanides/biguanides (phenformin and galegine [isoamylene guanidine]), and piericidin A on glycerol-derived gluconeogenesis and cytosolic redox state in liver slices, as well as their effects on $[^{13}C_3]$glycerol incorporation into $[^{13}C_3]$glucose in awake rats with indwelling intraportal catheters. Finally, we investigated a mechanism of metformin/phenformin/galegine action through cytochrome c oxidase (complex IV)-mediated inhibition of GPD2 activity, which, in turn, can explain guanide/biguanide effects to increase the hepatic cytosolic redox state and reduce glycerol-derived hepatic gluconeogenesis and glycerol-3-phosphate (G3P)-dependent mitochondrial oxidation.

Results

Redox-Dependent Inhibition of Gluconeogenesis with Metformin Is Not Replicated by Complex I Inhibition. To assess the substrate-selective effect of guanides/biguanides on hepatic gluconeogenesis, we prepared precision-cut liver slices from healthy overnight-fasted rats (34). Increased cytosolic redox selectively inhibits gluconeogenesis from redox-dependent substrates (lactate and glycerol), but not redox-independent substrates (alanine, dihydroxyacetone [DHA], and pyruvate) (20). As such, liver slices were incubated with gluconeogenesis medium containing glycerol or DHA and one of the following treatments: 0.01 µM piericidin A (complex I inhibitor), 0.1 µM potassium cyanide (KCN; complex IV inhibitor), 300 µM metformin, 200 µM phenformin, or 100 µM galegine. Rates of glucose production from glycerol were significantly reduced in liver slices treated with each of the three guanides/biguanides, while piericidin A had no effect, dissociating guanide/biguanide-induced inhibition of hepatic gluconeogenesis from complex I activity (Fig. 1A). Interestingly, complex IV inhibition with cyanide also reduced glucose production from glycerol (Fig. 1A).

Consistent with previous studies (20, 35–37), we also show that metformin, phenformin, and galegine treatment increased
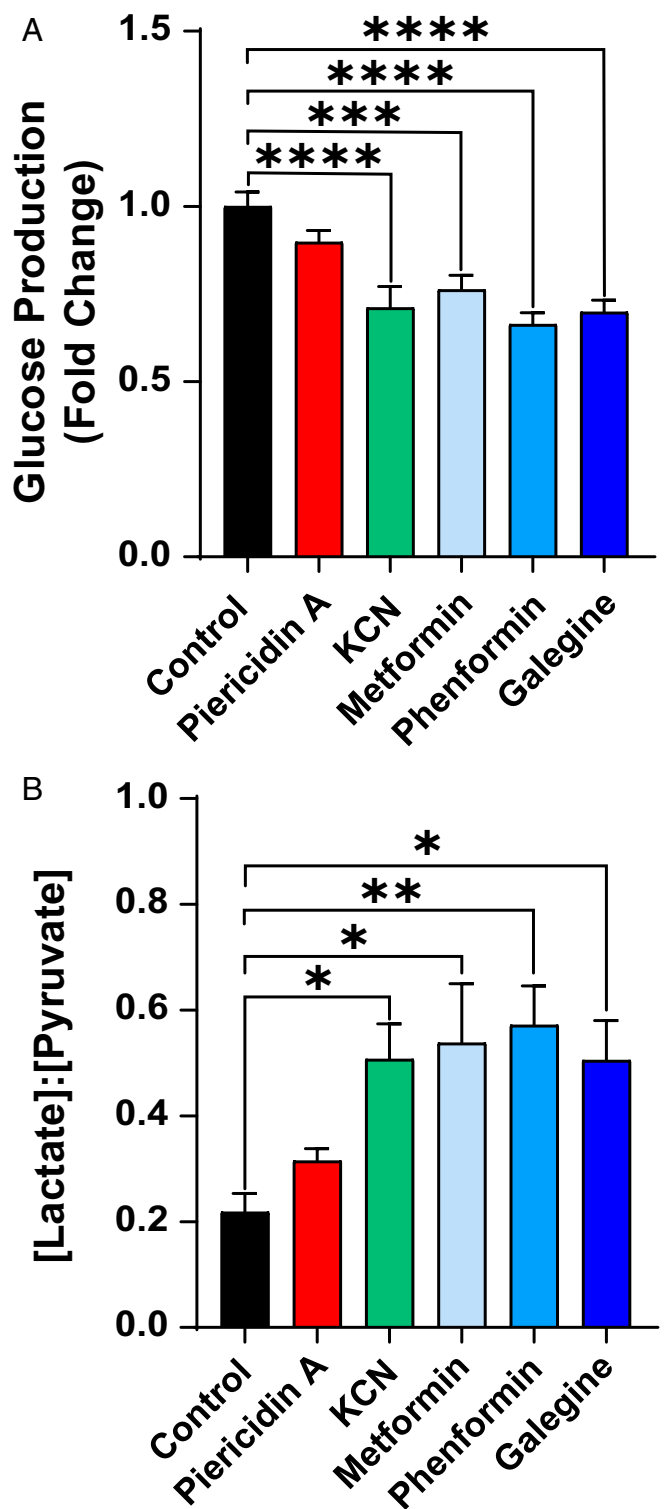
Fig. 1. Guanides/biguanides and cyanide, but not piericidin A, inhibit HGP and increase the hepatic cytosolic redox state in vitro. (A) Glucose production in rat liver slices incubated for 6 h in gluconeogenesis medium containing 100 µM glycerol and the indicated treatments: water (control), 0.01 µM piericidin A, 0.1 µM KCN, 300 µM metformin, 200 µM phenformin, or 100 µM galegine. Glucose release into the medium was normalized to frozen tissue weight and expressed as fold change from control. (B) [Lactate]:[pyruvate] ratio in rat liver slices treated as in A. Data are representative of six independent experiments and are shown as mean ± SEM. *$P < 0.05$; **$P < 0.01$; ***$P < 0.001$; ****$P < 0.0001$ (by one-way ANOVA).

cytosolic redox in liver slices, as indicated by an increased [lactate]:[pyruvate] ratio (Fig. 1*B*). To determine whether guanides/biguanides may be acting through complex I inhibition, we compared the [lactate]:[pyruvate] ratio in guanide/biguanide-treated liver slices with piericidin A treatment and found that, in contrast to the guanides/biguanides, piericidin A had no effect on the [lactate]:[pyruvate] ratio (Fig. 1*B*). However, consistent with a previous report (38), we observed an increased [lactate]:[pyruvate] ratio in slices incubated with KCN, similar to guanide/biguanide treatment. Taken together, these data do not support complex I inhibition as a mechanism of metformin action and implicate complex IV as a potential target of metformin.

We repeated this experiment with DHA instead of glycerol as the gluconeogenic substrate, and, as predicted, substitution with a nonreduced substrate (DHA) eliminated guanide/biguanide inhibition of gluconeogenesis (*SI Appendix*, Fig. S1*A*). Furthermore, we observed a similar substrate selectivity with KCN treatment, while piericidin A failed to alter rates of glucose production with either substrate (*SI Appendix*, Fig. S1*A*). DHA also abrogated guanide/biguanide- and cyanide-induced alterations in cytosolic redox, as the [lactate]:[pyruvate] ratio was unchanged in all treatment groups when DHA was substituted for glycerol (*SI Appendix*, Fig. S1*B*). In summary, these data demonstrate that guanide/biguanide inhibition of gluconeogenesis via increased cytosolic redox is incompatible with a complex I-dependent mechanism of action. We also show that complex IV inhibition reduces hepatic gluconeogenesis via a redox-dependent mechanism that mimics guanide/biguanide treatment.

Effects of Metformin, Phenformin, Galegine, and Piericidin A on In Vivo Glucose Metabolism. To compare the effects of guanides/biguanides and pieridicin A on glucose metabolism in vivo, we infused 30-h-fasted, hepatic glycogen-depleted rats with 100 mg/[kg-h] metformin, 50 mg/[kg-h] phenformin, 25 mg/[kg-h] galegine, 0.1 mg/[kg-h] piericidin A, or saline (control). Because guanides/biguanides are taken orally and accumulate to a high degree in the liver, each compound was infused via a chronic indwelling portal vein catheter over 1 h (39–41). Plasma glucose concentrations were reduced following acute intraportal infusions of phenformin and galegine treatment, while piericidin A surprisingly increased plasma glucose concentrations (Fig. 2*A*). Plasma glucose concentrations were unchanged during the metformin intraportal infusion, consistent with its tendency to have minimal glucose-lowering effects in normoglycemic individuals and greater glucose-lowering effects in individuals with poorly controlled T2D (8, 27–29, 42). Intraportal infusions of metformin, phenformin, or galegine significantly increased plasma lactate concentrations compared to the saline control, suggesting that they all promote an increase in anaerobic glycolysis (Fig. 2*B*). Intraportal infusions of piericidin A
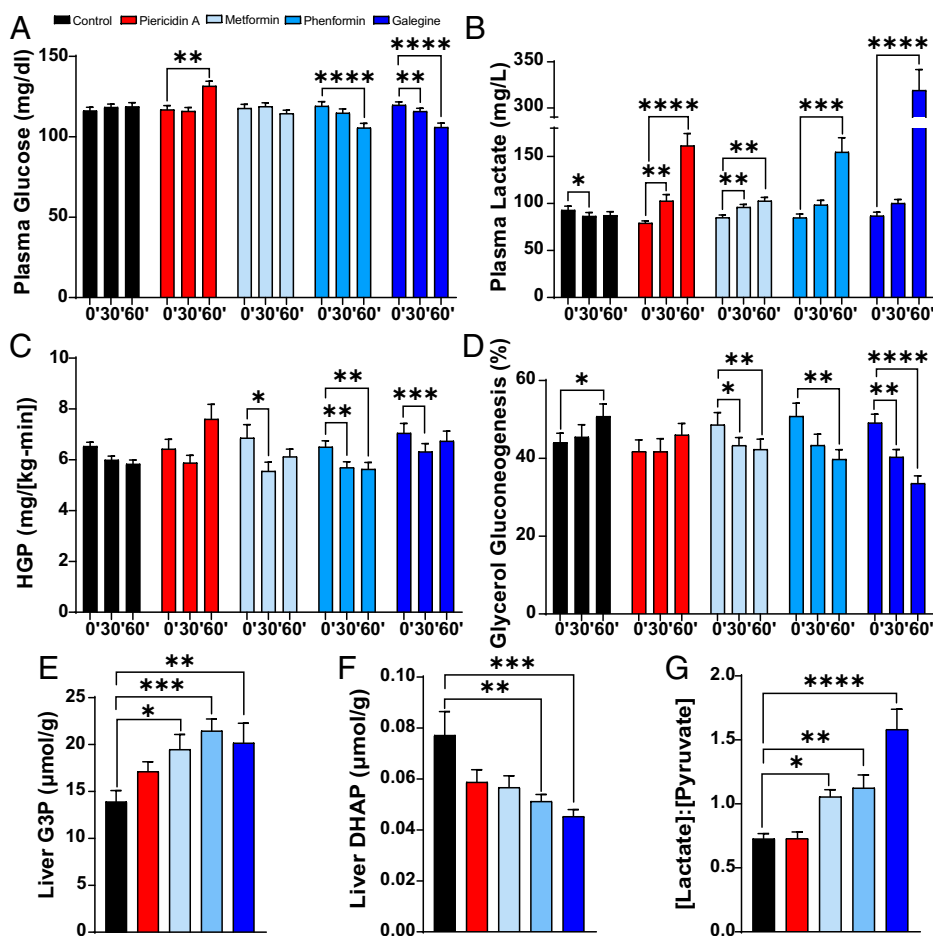
Fig. 2. Metformin, phenformin, and galegine, but not piericidin A, inhibit glycerol-derived gluconeogenesis and increase the hepatic cytosolic redox state in vivo. (*A–C*) Plasma glucose concentrations (*A*), plasma lactate concentrations (*B*), and HGP rate (*C*) during an acute portal infusion of saline (control), 0.1 mg/[kg-h] piericidin A, 100 mg/[kg-h] metformin, 50 mg/[kg-h] phenformin, or 25 mg/[kg-h] galegine. (*D–G*) Percent contribution of glycerol to total hepatic gluconeogenesis (*D*), hepatic G3P content (*E*), hepatic DHAP content (*F*), and hepatic [lactate]:[pyruvate] ratio (*G*) in rats treated as in *A*. Data are mean ± SEM. *n* = 12 to 19 per group. *$P < 0.05$; **$P < 0.01$; ***$P < 0.001$; ****$P < 0.0001$ (by ANOVA).

LaMoia et al.
Metformin, phenformin, and galegine inhibit complex IV activity and reduce glycerol-derived gluconeogenesis

PNAS | 3 of 9
https://doi.org/10.1073/pnas.2122287119

also increased plasma lactate concentrations (Fig. 2B), confirming that the infusion rate chosen (0.1 mg/[kg-h]) was sufficient to inhibit complex I activity and impair oxidative metabolism (43). However, while metformin (at 30 min), phenformin (at 30 and 60 min), and galegine (at 30 min) all reduced HGP, piericidin A had no effect on HGP (Fig. 2C), providing further evidence that complex I inhibition is inconsistent with the glucose-lowering effects of metformin at clinically relevant doses.

Guanides/Biguanides Reduce Glycerol-Derived Gluconeogenesis through a Redox-Dependent Mechanism. To evaluate the effects of guanides/biguanides on glycerol-derived gluconeogenesis, a continuous infusion of $[^{13}C_3]$glycerol and $[3\text{-}^3H]$glucose was administered through the arterial catheter and was maintained throughout the intraportal infusion of the indicated treatments. Using $[^{13}C_3]$glycerol, we were able to calculate the fractional contribution of glycerol to total HGP throughout the intraportal infusion of metformin, phenformin, galegine, or piericidin A by analyzing plasma $[^{13}C]$glucose and $[^{13}C]$glycerol enrichments. Intraportal infusions of metformin, phenformin, and galegine reduced fractional contributions of glycerol to hepatic gluconeogenesis by 13% ($P < 0.01$), 22% ($P < 0.01$), and 32% ($P < 0.0001$), respectively, while this inhibitory effect was absent following piericidin A infusion (Fig. 2D). Furthermore, intraportal infusions of metformin, phenformin, and galegine reduced absolute rates of glycerol-derived glucose production, while piericidin A demonstrated a strong tendency ($P = 0.07$) to promote an ~25% increase in glycerol-derived gluconeogenesis (*SI Appendix*, Fig. S2B). Consistent with guanide/biguanide inhibition of GPD2 activity, we also observed increased liver G3P and decreased liver DHAP content with guanides/biguanides, while this effect was absent with piericidin A treatment (Fig. 2 E and F).

We also examined the effects of intraportal infusions of metformin, phenformin, galegine, and piericidin A on hepatic cytosolic redox state at the end of the study, as reflected by the liver [lactate]:[pyruvate] ratio. Consistent with our observations in liver slices, metformin, phenformin, and galegine increased the liver [lactate]:[pyruvate] ratio, while complex I inhibition with piericidin A treatment had no effect on the hepatic [lactate]: [pyruvate] ratio (Fig. 2G).

Metformin, Phenformin, and Galegine Inhibit Complex IV Activity at Clinically Relevant Concentrations. Guanides/biguanides are widely reported to bind metals, such as copper and iron, which are present in several complexes of the ETC (44–46). Thus, we hypothesized that metformin's metal-binding properties might be modulating ETC activity. We have shown here that complex I is an unlikely target to explain the glucose-lowering effects of guanides/biguanides; however, as described above, complex IV inhibition with KCN increases the [lactate]:[pyruvate] ratio in liver slices, leading to reduced glucose production from glycerol, which is consistent with the glucose-lowering effect of guanides/biguanides (Fig. 1). Using a Clark-type oxygen electrode, we measured complex IV activity in the presence of increasing concentrations of metformin, phenformin, or galegine (Fig. 3). Consistent with the order of potency of guanides/biguanides (galegine > phenformin > metformin), galegine inhibited complex IV activity at a concentration of ≥300 μM, followed by phenformin at a concentration of ≥400 μM, and, finally, metformin, which required a concentration of ≥500 μM to induce significant inhibition of complex IV activity (Fig. 3A). This experiment was performed at cytosolic pH (7.4); however, metformin primarily accumulates in the mitochondrial matrix, where the pH is ~7.8 to 7.9. So, we repeated this experiment at pH 7.9 to determine whether this would impact the effects of guanides/biguanides on complex IV activity. Interestingly, mitochondrial matrix pH reduced the minimum concentration required to attenuate complex IV activity: We observed a
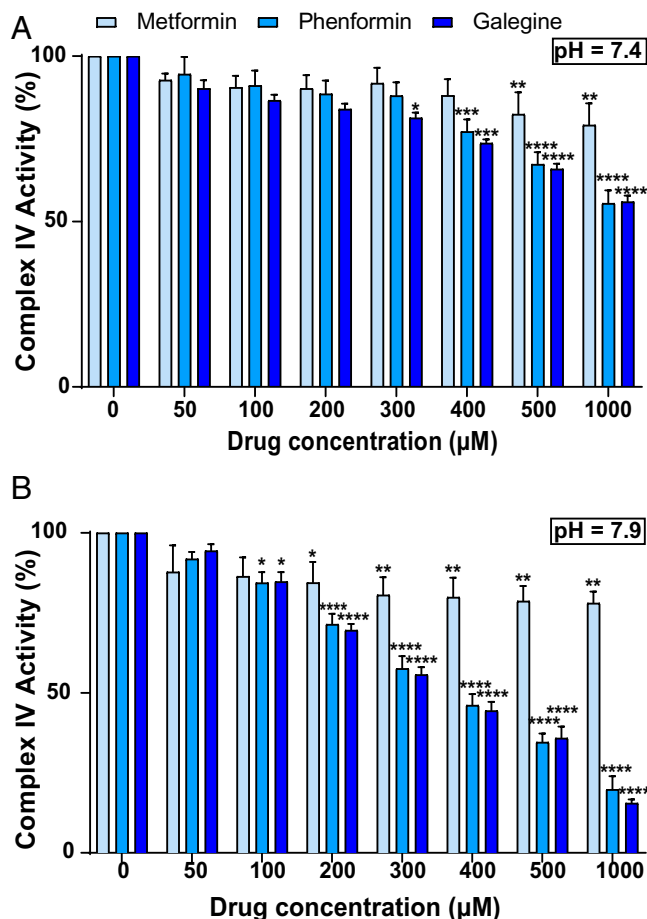

Fig. 3. Metformin, phenformin, and galegine inhibition of complex IV activity is pH-dependent. Complex IV activity was measured after injection of 50 μM to 1 mM of each drug at pH 7.4 (A) or pH 7.9 (B). Data are mean ± SEM. *n* = 3 or 4 per group. *P < 0.05; **P < 0.01; ***P < 0.001; ****P < 0.0001 (by ANOVA).

significant inhibitory effect with 100 μM phenformin and galegine and 200 μM metformin (Fig. 3B). These hepatic concentrations of phenformin and metformin are within the range of concentrations observed in the liver following oral administration of clinically relevant doses of these guanides/biguanides (20, 39). This effect was dose-dependent with phenformin and galegine, while metformin inhibition of complex IV activity plateaued at ~20% inhibition.

Effects of Metformin, Phenformin, and Galegine on Complex IV Spectral Absorption. Consistent with the effects of metformin, phenformin, and galegine to inhibit complex IV activity, we also found that the addition of metformin, phenformin, and galegine affected the spectral absorption of complex IV (Fig. 4). Complex IV has a typical absorption peak derived from heme moieties at ~420 nm. Here, we show that the addition of metformin, phenformin, or galegine induced spectrum changes around 420 nm, indicating that guanides/biguanides directly bind to complex IV. Furthermore, these changes were more pronounced at pH 7.9 compared to pH 7.4, reflecting differences in binding manner or intensity that are pH-dependent, similar to the pH-dependent effect of guanides/biguanides on complex IV activity (Fig. 3). Taken together, these data provide additional support for direct interactions between guanides/biguanides and complex IV.
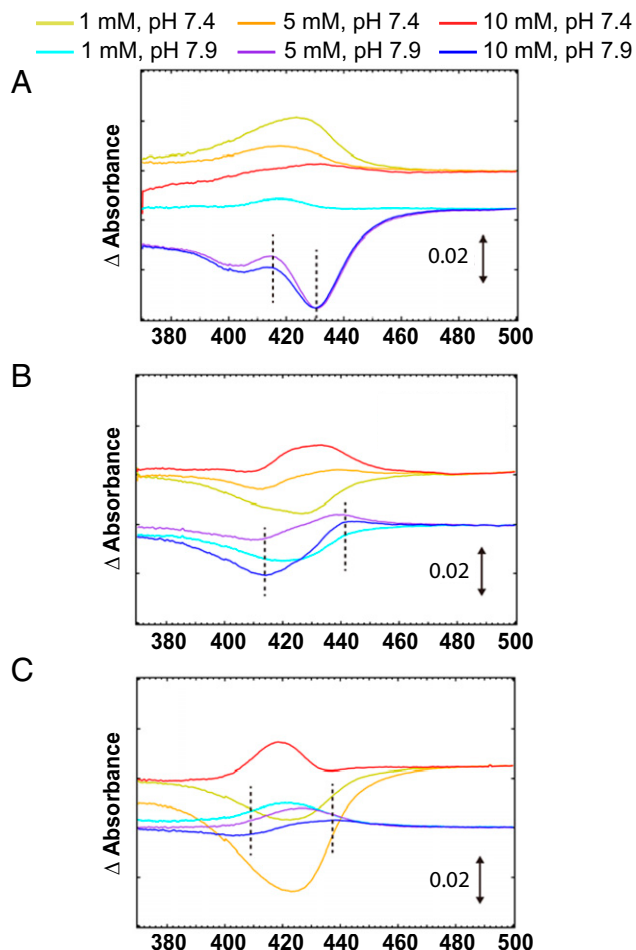
Fig. 4. Guanides/biguanides alter the difference spectrum of complex IV. The difference spectrums at 60 min after mixing complex IV and metformin (*A*), phenformin (*B*), or galegine (*C*). Each trace is a difference spectrum against the spectrum of complex IV without guanide/biguanides and guanide/biguanides without complex IV. Two peaks meaning the peak shift induced by the presence of guanide/biguanide are indicated by dashed lines.

Complex IV-Mediated Inhibition of G3P-Dependent Respiration. We next wanted to understand the potential mechanism by which guanide/biguanide/cyanide inhibition of complex IV activity leads to reductions in glycerol-derived gluconeogenesis. In this regard, Hargreaves et al. (47) demonstrated that complex IV inhibition leads to a backlog in the ETC, resulting in inhibition of upstream complexes II and III. Given that GPD2 activity is tightly coupled to complex II activity, we hypothesized that guanide/cyanide inhibition of complex IV backlogs the ETC and indirectly inhibits GPD2 activity. To address this hypothesis, we measured mitochondrial respiration from G3P, the primary substrate for GPD2 and an intermediate for glycerol entry to the gluconeogenic pathway. Consistent with a previous report (48), we found that acute low-dose cyanide treatment inhibits G3P-stimulated respiration in isolated rat mitochondria (Fig. 5). Similarly, and consistent with our hypothesis, we found that metformin, phenformin, and galegine also inhibited G3P-stimulated respiration under the same conditions.

Discussion

Several distinct mechanisms of metformin action have been proposed, with complex I inhibition being the most extensively studied (14–16, 18, 49–53). While this mechanism is still widely accepted, we and others have questioned its clinical relevance

due to the suprapharmacological (millimolar) metformin concentrations required to observe complex I inhibition (40) and the absence of changes in complex I activity with clinically relevant concentrations of metformin (20, 54, 55).

To our knowledge, complex I inhibition has not been convincingly shown to replicate the therapeutic effects of metformin in vivo. The few studies that examine hepatic complex I inhibition primarily use rotenone, which has numerous off-target effects, as evidenced by the specific use of rotenone treatment as a rodent model of Parkinson's disease (56). Thus, in this study, we used piericidin A, which is a much more selective inhibitor of complex I activity, to determine whether complex I inhibition replicates the effects of metformin on glucose homeostasis both in vitro and in vivo. In contrast to guanides/biguanides, we report that acute portal administration of piericidin A rapidly increased plasma glucose concentrations, which
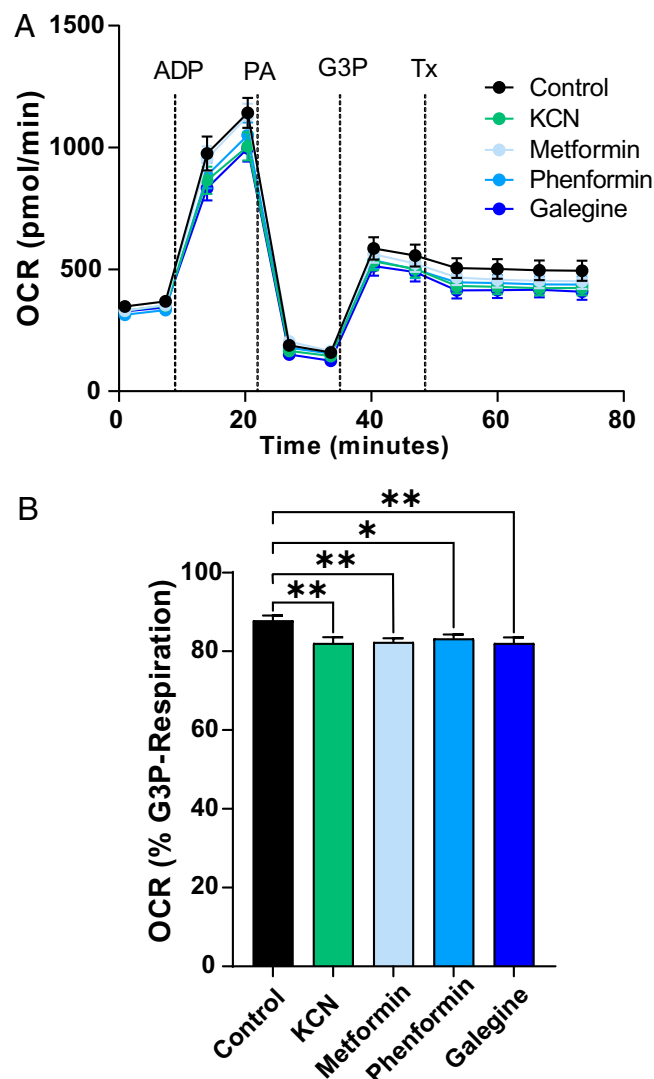
Fig. 5. Complex IV inhibition with metformin, phenformin, galegine, and KCN reduces respiration from G3P in isolated mitochondria. (*A*) Representative trace of oxygen consumption in isolated rat mitochondria. Dashed line indicates injection of the indicated compounds. PA, 1 μM piericidin A; Tx, treatment (control, 200 μM galegine, or 10 μM KCN). (*B*) Quantification of mitochondrial respiration following injection of G3P and the indicated treatments. Data are normalized to basal respiration from G3P prior to treatment injection. Data are mean $\pm$ SEM and representative of 16 independent experiments. *$P < 0.05$; **$P < 0.01$ (by ANOVA).

LaMoia et al.
Metformin, phenformin, and galegine inhibit complex IV activity and reduce glycerol-derived gluconeogenesis

PNAS | 5 of 9
https://doi.org/10.1073/pnas.2122287119

was likely due to the tendency for piericidin A to increase rates of HGP (Fig. 2). We also found that while plasma lactate concentrations were increased by piericidin A administration, consistent with whole-body transition to anaerobic glycolytic metabolism, the liver [lactate]:[pyruvate] ratio was unaffected by piericidin A treatment in vivo or in vitro (Figs. 1B and 2G). This is in contrast to metformin, phenformin, or galegine treatment, which uniformly decrease rates of HGP, while also increasing plasma lactate concentrations and the hepatic cytosolic redox state, as reflected by an increase in the liver [lactate]:[pyruvate] ratio (Fig. 2), as we and others have previously reported (20, 21). Taken together, these results demonstrate that the glucose-lowering effects of metformin, phenformin, and galegine are inconsistent with complex I inhibition.

Glycerol enters the gluconeogenic pathway via GPD2-mediated conversion of G3P to DHAP, and, consistent with metformin inhibition of GPD2, we show that acute intraportal administration of metformin, phenformin, and galegine significantly reduces the fractional contribution of glycerol to gluconeogenesis in vivo (Fig. 2D). Further, recent studies have shown that glycerol contribution to gluconeogenesis during a prolonged fast is higher than previously thought, accounting for ~50% of gluconeogenic flux in 18-h-fasted mice (57), which is similar to the values we report in 30-h-fasted rats. In the context of human obesity and/or T2D, glycerol contributions to gluconeogenesis are significant due to dysregulated WAT lipolysis, which would explain the greater glucose-lowering effects of metformin in patients with poorly controlled T2D, as opposed to normoglycemic individuals (8, 27–29, 42). In the present study, 30-h-fasted rats were used to mimic dysregulated WAT lipolysis seen in poorly controlled T2D models.

Metformin is consistently reported to increase cytosolic redox, leading to reduced lactate dehydrogenase (LDH) activity and selective inhibition of gluconeogenesis from lactate (12, 20–22, 25, 35, 36, 58, 59). Alshawi and Agius (37) recently proposed that low concentrations of metformin inhibit the malate–aspartate shuttle, not the glycerophosphate shuttle (GPD2), leading to the observed increased cytosolic redox. While it is true that inhibition of the malate–aspartate shuttle would also be expected to increase cytosolic redox and potentially reduce lactate conversion to glucose, metformin's ability to decrease glycerol-derived gluconeogenesis, as shown in the present study, is inconsistent with inhibition of the malate–aspartate shuttle and suggests that GPD2 mediates metformin's glucose-lowering effects.

Based on the ability of guanides/biguanides to act as a Schiff base and bind metal ions such as copper and iron, which are both present in complex IV, we hypothesized that metformin, phenformin, and galegine may be modulating the activity of this metalloprotein (44–46). Previous studies have shown that complex IV inhibition with KCN backlogs the ETC, specifically complexes II and III (47), and increases the liver [lactate]:[pyruvate] ratio (38). In the present study, we show that metformin, phenformin, and galegine dose-dependently reduce complex IV activity at clinically relevant concentrations (Fig. 3), and, in contrast to complex I inhibition with piericidin A, KCN reduces HGP via increased cytosolic redox, which is in agreement with metformin's therapeutic effects (Fig. 1). This result is also consistent with the glucose-lowering effects of triphenyl phosphonium–thiazole, another complex IV inhibitor, in aged and diabetic mice (60). Metformin's inhibitory effect on complex IV plateaued at ~20% inhibition, while higher concentrations of phenformin and galegine increasingly inhibited complex IV activity (~80% and ~85%, respectively). This is consistent with the markedly greater risk of lactic acidosis with phenformin, which ultimately led to phenformin's withdrawal from clinical use, and suggests that guanide/biguanide inhibition of complex IV may also promote an increase in non-insulin-stimulated
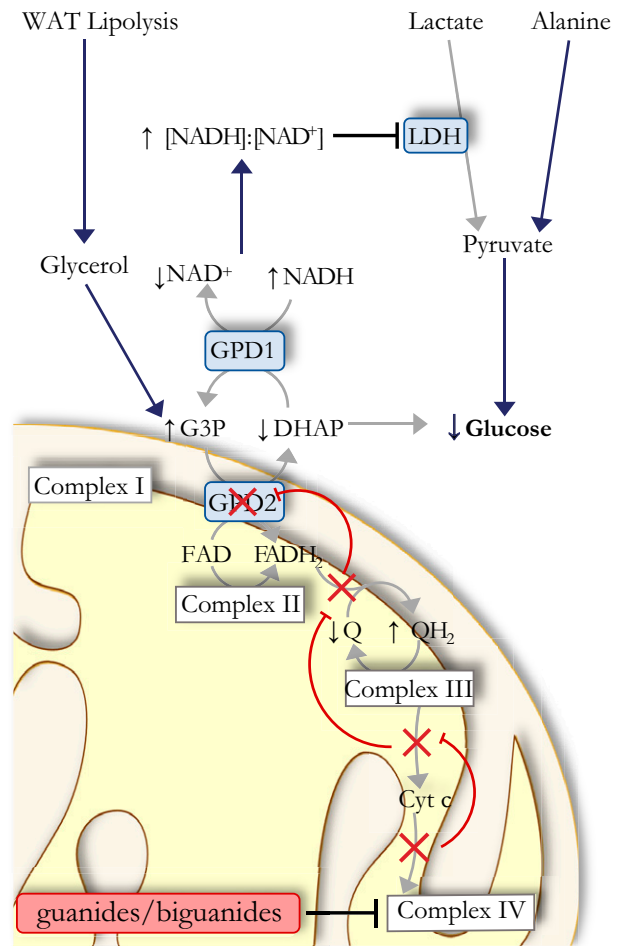

Fig. 6. Overview of proposed mechanism of guanide/biguanide action. The glycerophosphate shuttle transfers reducing equivalents between the mitochondria and the cytoplasm via glycerol-3-phosphate dehydrogenase 1 (GPD1) and GPD2. GPD2 converts G3P to DHAP and simultaneously transfers electrons to FAD, generating $FADH_2$. Electrons enter the ETC via transfer from $FADH_2$ to ubiquinone to generate ubiquinol. Ubiquinol is oxidized back to ubiquinone by complex III, which transfers electrons to oxidized cytochrome c. Reduced cytochrome c is subsequently reoxidized by complex IV. When guanides/biguanides bind to and inhibit complex IV, this leads to a backlog of the ETC and inhibition of electron transport by complex III, complex II, and GPD2. This prevents the conversion of G3P to DHAP, thus inhibiting glycerol-derived gluconeogenesis. Furthermore, dysregulation of the glycerophosphate shuttle leads to excess reducing equivalents in the cytosol (increased $[NADH]:[NAD^+]$), which decreases lactate conversion to pyruvate by LDH and lactate-derived gluconeogenesis. cyt c, cytochrome c; FAD, flavin adenine dinucleotide; Q, ubiquinone; QH_2, ubiquinol.

glucose uptake and anaerobic glycolysis. We also show that guanides/biguanides alter the spectral absorption of complex IV, suggesting that they modulate complex IV activity via direct interaction with the enzyme (Fig. 4). However, additional structural studies are necessary to identify a precise binding site.

The complex IV inhibitory effect and spectrum changes we observed are more pronounced at mitochondrial matrix pH, where metformin, phenformin, and galegine likely bind to complex IV (Fig. 4): It has been estimated that metformin and related compounds accumulate in the mitochondrial matrix due to the mitochondrial membrane potential, which is negative on the inside and attracts positively charged molecules (61). Because the liver takes up the vast majority of circulating

metformin from the portal vein, with metformin concentrations in the range of 40 to 70 μM (20, 39, 40), and because the drug accumulates in the mitochondrial matrix, local mitochondrial matrix concentrations should easily exceed the minimally effective concentrations leading to complex IV inhibition, as we report here. In support of this, we show that acute intraportal infusion of guanides/biguanides leads to liver metformin, phenformin, or galegine concentrations in the range of 110 to 240 μM and plasma concentrations in the range of 20 to 70 μM (*SI Appendix*, Fig. S2 *D–F*).

Taken together, we propose an indirect mechanism of GPD2 inhibition, in which downstream attenuation of complex IV activity by metformin backlogs the ETC, leading to a decrease in the ubiquinone pool—the electron acceptor of GPD2—and thus to indirect inhibition of GPD2 (Fig. 6). To directly test the validity of this mechanism, we evaluated G3P-stimulated respiration in isolated rat liver mitochondria treated with KCN or guanides/biguanides, and, in agreement with a previous report (48), we found that, in fact, complex IV inhibition was sufficient to reduce G3P-dependent oxygen consumption rate (OCR), likely through inhibition of GPD2 activity (Fig. 5). While we and others have previously demonstrated that guanides/biguanides inhibit GPD2 activity in vitro (21, 22, 62), other studies have observed no effect on GPD2 activity (37, 63). Notably, GPD2 activity assays are often performed in the presence of millimolar concentrations of KCN or other complex IV inhibitors, which, according to the mechanism we propose, may mask the effects of metformin on GPD2 activity (63). Furthermore, disruption of the ETC would also impact this pathway, leading to variability based on the prep used (e.g., intact mitochondria vs. mitochondrial lysates), potentially explaining the discordant effects reported in the literature (21, 22, 37, 48, 63).

In summary, we demonstrate that metformin, phenformin, and galegine inhibit complex IV activity at clinically relevant concentrations, leading to inhibition of GPD2 activity, increased cytosolic redox, and selective inhibition of glycerol-derived hepatic gluconeogenesis both in vitro and in vivo (Fig. 6). In contrast, inhibition of complex I activity with pieridicin A did not replicate any of these effects in vitro or in vivo, thus making complex I an unlikely clinically meaningful target for metformin action. However, the proposed mechanism reconciles several questions related to the mechanism of metformin action, including metformin's remarkable safety profile, where, in contrast to the other guanide/biguanides, metformin's inhibitory effect on complex IV plateaus at ~20%, as well as why metformin's glucose-lowering effects are greater in obese, poorly controlled T2D patients, who typically have increased rates of WAT lipolysis, compared to normoglycemic individuals due to selective inhibition of glycerol-derived gluconeogenesis.

Materials and Methods

Animal Studies. All protocols were approved by the Institutional Animal Care and Use Committee of Yale University. Healthy male Sprague–Dawley rats weighing 350 to 450 g were ordered from Charles River Laboratories and maintained on regular chow and water ad libitum. Upon arrival, rats were housed on a 12-h light/dark cycle at ~25 °C and underwent surgery under isoflurane anesthesia to place catheters in the jugular vein, common carotid artery, and portal vein. Animals were randomly allocated to treatment groups, and the studies were performed unblinded. All studies were performed in awake, unrestrained animals. Arterial catheters were used for tracer infusions (0.1 μCi/min [3-^{3}H]glucose and 10 μmol/[kg-min] [^{13}C$_3$]glycerol), portal catheters were used for treatment administration (100 mg/[kg-h] metformin, 50 mg/[kg-h] phenformin, 25 mg/[kg-h] galegine, 0.1 mg/[kg-h] pieridicin A, or saline), and venous catheters were used for blood sampling. Following a 30-h fast, rats were given a continuous infusion of [3-^{3}H]glucose and [^{13}C$_3$]glycerol for 3 h. A portal infusion of saline, metformin, phenformin, galegine, or pieridicin A was maintained for the last hour. At the end of the study, rats were anesthetized by intravenously administered pentobarbital, and tissues were collected and immediately snap-frozen in liquid nitrogen.

Blood was sampled at 0, 30, and 60 min following the beginning of the portal infusion. Plasma glucose and lactate were measured immediately on a YSI 2700 Biochemistry Analyzer.

Liver Slices. The method described by de Buettner et al. (34) was used with the following modifications. Male Sprague–Dawley rats were fasted overnight (~16 h) and euthanized via isoflurane inhalation, and the liver was collected. The liver was rinsed with ice-cold KHB (110 mM NaCl, 4.6 mM KCl, 1.2 mM CaCl$_2$, 2 mM MgSO$_4$, and 1.4 mM NaH$_2$PO$_4$) and then cored to 8-mm-diameter cylinders (Alabama R&D catalog nos. MP0144 and MD5000). Cores were sliced to 250-μm thickness and kept in ice-cold KHB. Two slices were incubated in each well of a 24-well plate with 0.5 mL of gluconeogenesis medium (Dulbecco's Modified Eagle Medium without glucose, 45 mM NaHCO$_3$, 0.5% fatty acid-free bovine serum albumin (BSA), 10 mM Hepes, and 100 μM glycerol or 100 μM DHA) at 37 °C for 6 h, and medium was sampled every 90 min. After 6 h, slices were snap-frozen in liquid nitrogen, and medium was collected. Glucose in the medium was immediately measured (Sekisui Glucose SL Assay). Glucose production was normalized to frozen tissue weight. Liver slice [lactate]:[pyruvate] was determined as described below.

Complex IV Activity Assay. Purified bovine liver complex IV was diluted to a concentration of 3 μM, and cardiolipin (Sigma-Aldrich) was added to a 40:1 cardiolipin:complex IV molar ratio. The enzyme was dialyzed (molecular mass cutoff: 12,000 to 14,000 Da) in dialysis buffer (10 mM K-Hepes, pH 7.4, 40 mM KCl, and 1% Tween 20, supplemented with 0.2 mM ATP). Oxygen consumption was measured via Clark-type oxygen electrode (Oxygraph system; Hansatech) at a final concentration of 45 nM liver complex IV in a total volume of 200 μL of measuring buffer (10 mM K-Hepes, 40 mM KCl, and 1% Tween 20) at pH 7.4 or 7.9 as indicated. Ascorbate (20 mM) was added as an electron donor for cytochrome *c*. Purified cytochrome *c* (Sigma-Aldrich; 10 μM) was injected into the air-tight oxygen electrode chamber. Each drug was titrated into the chamber at the concentrations indicated.

Mitochondrial Respiration. Mitochondria were prepared immediately before each study carried out on a Seahorse Bioscience XF24 Analyzer. Liver was rapidly excised from a fed rat anesthetized under isoflurane. Liver was then homogenized in mitochondrial assay solution (70 mM sucrose, 220 mM mannitol, 5 mM KH$_2$PO$_4$, 5 mM MgCl$_2$, 2 mM Hepes, and 1 mM ethylene glycol-*bis*(β-aminoethyl ether)-N,N,N′,N′-tetraacetic acid). Mitochondria were purified by differential centrifugation, and the mitochondrial pellet was used for respiration studies in mitochondrial assay solution without BSA (final concentration 0.5 mg/mL mitochondrial protein). All reagents were diluted in mitochondrial assay solution without BSA and loaded into the ports of the flux plate (port A: 2 mM ADP; port B: 1 μM pieridicin A; port C: 40 mM G3P; port D: treatment indicated). The following concentrations were used for each treatment: mitochondrial assay solution (control), 200 μM metformin, 200 μM phenformin, 200 μM galegine, or 1 μM KCN.

Absorbance Spectrum Analysis. Complex IV sample purified from bovine heart as described (64) was diluted to a concentration of 10 μM with 100 mM sodium phosphate buffer (pH 7.4 or 7.9) containing 0.2% (weight [wt]/wt) decylmaltoside. The absorbance spectrum of complex IV with or without guanide/biguanides between 250 and 700 nm was measured every 10 min for 60 min at 20 °C by using a Jasco V-630 spectrometer equipped with a temperature-controlled cell holder. The difference spectrum was calculated by subtracting the absorbance spectrum of complex IV without guanide/biguanides and guanide/biguanides without complex IV from that of complex IV with guanide/biguanides at each time point.

Metabolite Measurements.

Gas chromatography-mass spectrometry analysis of pyruvate content. The method described by Young et al. (65) was used with the following modifications. Frozen liver tissue was homogenized in 5× volume (vol) methanol/water (50%, vol/vol) containing 0.05 μmol of d3 pyruvate (Cambridge Isotope, catalog no. DLM-6068-PK) and centrifuged at max speed for 10 min at 4 °C. The supernatant was collected and dried under nitrogen gas. The dried sample was dissolved in methoxamine, sonicated for 5 min, and heated at 40 °C for 90 min. *N*-methyl-*N*-(tert-butyldimethylsilyl)trifluoroacetamide plus 1% tert-butyldimethylchlorosilane was added, and samples were heated at 70 °C for 30 min. Pyruvate concentration was calculated via gas chromatography-mass spectrometry (GC-MS) (electron-ionization mode; pyruvate: retention time ~3.25, *m/z* 174 [*m*], … 177 [*m* + 3]) using peak area ratios of the metabolites vs. the internal standard.

GC-MS analysis of glycerol and glucose. Plasma samples were deproteinized by using Ba(OH)$_2$ and ZnSO$_4$, dried, and derivatized with 1:1 acetic anhydride:pyridine. After heating to 65 °C for 30 min, the reaction was quenched with

methanol. Glycerol and glucose were determined by GC-MS (chemical-ionization mode; glycerol: retention time ~2.85, m/z 219 [m], 222 [$m + 3$]; glucose: retention time ~7.8, 331 [m], 332 [$m + 1$], ... 337 [$m + 6$]). Percent gluconeogenesis from glycerol was calculated as follows:

$$\frac{[m + 3]glucose}{2^*[m + 3]glycerol}.$$

Liquid chromatography–tandem MS quantitation of G3P and DHAP. Plasma or frozen tissue was added to 0.75 mL of prechilled acetonitrile/water (60:40, vol/vol) solution containing 0.04 μmol of the internal standard (D_4-taurine). Samples were homogenized (Qiagen Tissue Lyser), followed by centrifugation (4,000 rpm) at 4 °C for 10 min. The supernatant was filtered with a nanosep 100K centrifugal device (Pall Life Science) before liquid chromatography–tandem MS (LC-MS/MS) analysis. The LC-MS/MS analysis was performed on an Applied Biosystems 6500 QTRAP, equipped with a Shimadzu ultrafast LC system. The chemical structures of the internal standards are not identical to the targeted metabolites; thus, standard curves are needed for G3P, DHAP, galegine, and piericidin A.

An electrospray ionization (ESI) source in negative mode was used for G3P, DHAP, and D_4-taurine analysis. The methanol/aqueous (1/1) solutions of G3P, DHAP, and D_4-taurine were used to optimize their ion-pair-dependent parameters, including: curtain gas (14 V), collision gas (medium), ionization potential (−2,000 V), probe temperature (500 °C), ion source gas 1 (60 V), ion source gas 2 (60 V), and entrance potential (EP) (10 V). The other compound-dependent parameters are summarized in *SI Appendix*, Table S1 for G3P, DHAP, and D_4-taurine. Metabolites (G3P and DHAP) and internal standard (D_4-taurine) were monitored with multiple reaction monitoring (MRM) mode. A Thermo Hypercarb high-performance LC (HPLC) column (100 mm × 4 mm) was used with a mixed solvent of 10 mM ammonium acetate aqueous solution and pure acetonitrile. Metabolite concentrations were calculated from peak area ratios of the metabolites vs. their internal standards, according to the corresponding calibration curves.

LC-MS/MS quantitation of metformin, phenformin, and galegine. Plasma or frozen tissue was added to 0.1 mL of water with 0.1% formic acid and 0.15 mL of methanol containing 0.4 μmol of internal standard (D_6-metformin for metformin and galegine and D_5-phenformin for phenformin). Plasma samples were vortexed, and tissue samples were homogenized followed by centrifugation. The supernatant was dried under a stream of nitrogen gas, resuspended with 0.3 mL of water with 0.1% formic acid, and filtered with a nanosep 100K centrifugal device before LC-MS/MS analysis.

An ESI source with a positive mode was used for the analysis of metformin, phenformin, and galegine, and the ion-pair-dependent parameters were

optimized. The optimized parameters are: curtain gas (14 V), collision gas (medium), ionization potential (5,000 V), probe temperature (450 °C), ion source gas 1 (60 V), ion source gas 2 (60 V), and EP (10 V). The other compound-dependent parameters were also summarized in *SI Appendix*, Table S1 for phenformin, galegine, and D_6-metformin. A C_8 reverse-phase LiChrosorb HPLC column (100 mm × 3 mm) was used with a mixed solvent of 10 mM ammonium acetate aqueous solution and pure acetonitrile. Concentrations were calculated from the peak area ratios of metformin, phenformin, and galegine vs. their internal standard, according to the corresponding calibration curves.

LC-MS/MS quantitation of piericidin A. For piericidin A, samples were homogenized in chloroform/methanol (2:1, vol/vol) containing 0.04 μmol of capsaicin. Samples were incubated on a shaker for 3 h at room temperature. H_2SO_4 was added (0.1 M final concentration), followed by centrifugation. The organic layer was collected and used for LC-MS/MS analysis.

An ESI source with a positive mode was used, and the ion-pair-dependent parameters were optimized. Capsaicin was used as the internal standard for the analysis, and the optimized parameters included curtain gas (20 V), collision gas (medium), ionization potential (5,500 V), probe temperature (450 °C), ion source gas 1 (55 V), and EP (10 V). A C_8 reversal-phase LiChrosorb HPLC column (100 mm × 3 mm) was used with a mixed solvent of 10 mM ammonium acetate aqueous solution and pure acetonitrile. Piericidin A and capsaicin were monitored with MRM mode. Piericidin A and capsaicin were measured with ion pairs of 416.2/398.3 and 306.2/182.1, respectively; the concentrations were calculated from the peak area ratios of piericidin A vs. capsaicin, according to the corresponding calibration curves.

Statistical Analysis. Comparisons were performed by using the unpaired two-tailed Student's t test (if two groups were compared) or ANOVA (if more than two groups were compared), with significance defined as $P < 0.05$. GraphPad Prism 9.0 was used for all statistical analysis. Data are presented as the mean ± SEM.

Data Availability. All study data are included in the article and/or *SI Appendix*.

1. C. J. Bailey, Metformin: Historical overview. *Diabetologia* **60**, 1566–1576 (2017).
2. P. King, I. Peacock, R. Donnelly, The UK prospective diabetes study (UKPDS): Clinical and therapeutic implications for type 2 diabetes. *Br. J. Clin. Pharmacol.* **48**, 643–648 (1999).
3. G. G. Graham *et al.*, Clinical pharmacokinetics of metformin. *Clin. Pharmacokinet.* **50**, 81–98 (2011).
4. L. S. Hermann, Metformin: A review of its pharmacological properties and therapeutic use. *Diabete Metab.* **5**, 233–245 (1979).
5. A. B. Iversen *et al.*, Results from ^{11}C-metformin-PET scans, tissue analysis and cellular drug-sensitivity assays questions the view that biguanides affects tumor respiration directly. *Sci. Rep.* **7**, 9436 (2017).
6. A. J. Scheen, Clinical pharmacokinetics of metformin. *Clin. Pharmacokinet.* **30**, 359–371 (1996).
7. P. Timmins, S. Donahue, J. Meeker, P. Marathe, Steady-state pharmacokinetics of a novel extended-release metformin formulation. *Clin. Pharmacokinet.* **44**, 721–729 (2005).
8. R. S. Hundal *et al.*, Mechanism by which metformin reduces glucose production in type 2 diabetes. *Diabetes* **49**, 2063–2069 (2000).
9. S. E. Inzucchi *et al.*, Efficacy and metabolic effects of metformin and troglitazone in type II diabetes mellitus. *N. Engl. J. Med.* **338**, 867–872 (1998).
10. K. Cusi, A. Consoli, R. A. DeFronzo, Metabolic effects of metformin on glucose and lactate metabolism in noninsulin-dependent diabetes mellitus. *J. Clin. Endocrinol. Metab.* **81**, 4059–4067 (1996).
11. R. A. DeFronzo, A. M. Goodman; The Multicenter Metformin Study Group, Efficacy of metformin in patients with non-insulin-dependent diabetes mellitus. *N. Engl. J. Med.* **333**, 541–549 (1995).
12. M. Stumvoll, N. Nurjhan, G. Perriello, G. Dailey, J. E. Gerich, Metabolic effects of metformin in non-insulin-dependent diabetes mellitus. *N. Engl. J. Med.* **333**, 550–554 (1995).
13. A. B. Johnson *et al.*, The impact of metformin therapy on hepatic glucose production and skeletal muscle glycogen synthase activity in overweight type II diabetic patients. *Metabolism* **42**, 1217–1222 (1993).
14. M. R. Owen, E. Doran, A. P. Halestrap, Evidence that metformin exerts its anti-diabetic effects through inhibition of complex 1 of the mitochondrial respiratory chain. *Biochem. J.* **348**, 607–614 (2000).
15. M.-Y. El-Mir *et al.*, Dimethylbiguanide inhibits cell respiration via an indirect effect targeted on the respiratory chain complex I. *J. Biol. Chem.* **275**, 223–228 (2000).
16. J. Cao *et al.*, Low concentrations of metformin suppress glucose production in hepatocytes through AMP-activated protein kinase (AMPK). *J. Biol. Chem.* **289**, 20435–20446 (2014).
17. M. Foretz *et al.*, Metformin inhibits hepatic gluconeogenesis in mice independently of the LKB1/AMPK pathway via a decrease in hepatic energy state. *J. Clin. Invest.* **120**, 2355–2369 (2010).
18. R. A. Miller *et al.*, Biguanides suppress hepatic glucagon signalling by decreasing production of cyclic AMP. *Nature* **494**, 256–260 (2013).
19. T. E. LaMoia, G. I. Shulman, Cellular and molecular mechanisms of metformin action. *Endocr. Rev.* **42**, 77–96 (2021).
20. A. K. Madiraju *et al.*, Metformin inhibits gluconeogenesis via a redox-dependent mechanism in vivo. *Nat. Med.* **24**, 1384–1394 (2018).
21. A. K. Madiraju *et al.*, Metformin suppresses gluconeogenesis by inhibiting mitochondrial glycerophosphate dehydrogenase. *Nature* **510**, 542–546 (2014).
22. L. Di Magno *et al.*, Phenformin inhibits hedgehog-dependent tumor growth through a complex I-independent redox/corepressor module. *Cell Rep.* **30**, 1735–1752.e7 (2020).
23. T. Mráček, Z. Drahota, J. Houštěk, The function and the role of the mitochondrial glycerol-3-phosphate dehydrogenase in mammalian tissues. *Biochim. Biophys. Acta* **1827**, 401–410 (2013).
24. F. D. Sistare, R. C. Haynes Jr., The interaction between the cytosolic pyridine nucleotide redox potential and gluconeogenesis from lactate/pyruvate in isolated rat hepatocytes. Implications for investigations of hormone action. *J. Biol. Chem.* **260**, 12748–12753 (1985).
25. J. Radziuk, Z. Zhang, N. Wiernsperger, S. Pye, Effects of metformin on lactate uptake and gluconeogenesis in the perfused rat liver. *Diabetes* **46**, 1406–1413 (1997).

8 of 9 | PNAS
https://doi.org/10.1073/pnas.2122287119

LaMoia et al.
Metformin, phenformin, and galegine inhibit complex IV activity and reduce glycerol-derived gluconeogenesis

26. E. I. M. Widén, J. G. Eriksson, L. C. Groop, Metformin normalizes nonoxidative glucose metabolism in insulin-resistant normoglycemic first-degree relatives of patients with NIDDM. *Diabetes* **41**, 354–358 (1992).

27. L. J. McCreight *et al.*, Metformin increases fasting glucose clearance and endogenous glucose production in non-diabetic individuals. *Diabetologia* **63**, 444–447 (2020).

28. N. Nurjhan, A. Consoli, J. Gerich, Increased lipolysis and its consequences on gluconeogenesis in non-insulin-dependent diabetes mellitus. *J. Clin. Invest.* **89**, 169–175 (1992).

29. I. Puhakainen, V. A. Koivisto, H. Yki-Järvinen, Lipolysis and gluconeogenesis from glycerol are increased in patients with noninsulin-dependent diabetes mellitus. *J. Clin. Endocrinol. Metab.* **75**, 789–794 (1992).

30. S. F. Previs, G. W. Cline, G. I. Shulman, A critical evaluation of mass isotopomer distribution analysis of gluconeogenesis in vivo. *Am. J. Physiol.* **277**, E154–E160 (1999).

31. R. J. Perry *et al.*, Hepatic acetyl CoA links adipose tissue inflammation to hepatic insulin resistance and type 2 diabetes. *Cell* **160**, 745–758 (2015).

32. M. C. Petersen, D. F. Vatner, G. I. Shulman, Regulation of hepatic glucose metabolism in health and disease. *Nat. Rev. Endocrinol.* **13**, 572–587 (2017).

33. M. C. Petersen, G. I. Shulman, Mechanisms of insulin action and insulin resistance. *Physiol. Rev.* **98**, 2133–2223 (2018).

34. R. Buettner *et al.*, Efficient analysis of hepatic glucose output and insulin action using a liver slice culture system. *Horm. Metab. Res.* **37**, 127–132 (2005).

35. A. J. M. Lewis *et al.*, Assessment of metformin-induced changes in cardiac and hepatic redox state using hyperpolarized[1-13C]pyruvate. *Diabetes* **65**, 3544–3551 (2016).

36. H. Qi *et al.*, Acute renal metabolic effect of metformin assessed with hyperpolarised MRI in rats. *Diabetologia* **61**, 445–454 (2018).

37. A. Alshawi, L. Agius, Low metformin causes a more oxidized mitochondrial NADH/NAD redox state in hepatocytes and inhibits gluconeogenesis by a redox-independent mechanism. *J. Biol. Chem.* **294**, 2839–2853 (2019).

38. S. J. Gee, C. E. Green, C. A. Tyson, Cyanide-induced cytotoxicity to isolated hepatocytes. *Toxicol. In Vitro* **4**, 37–45 (1990).

39. C. Wilcock, C. J. Bailey, Accumulation of metformin by tissues of the normal and diabetic mouse. *Xenobiotica* **24**, 49–57 (1994).

40. L. He, F. E. Wondisford, Metformin action: Concentrations matter. *Cell Metab.* **21**, 159–162 (2015).

41. L. C. Gormsen *et al.*, In vivo imaging of human 11C-metformin in peripheral organs: Dosimetry, biodistribution, and kinetic analyses. *J. Nucl. Med.* **57**, 1920–1926 (2016).

42. I. J. Neeland, C. Hughes, C. R. Ayers, C. R. Malloy, E. S. Jin, Effects of visceral adiposity on glycerol pathways in gluconeogenesis. *Metabolism* **67**, 80–89 (2017).

43. T. Mitsui, J.-i. Fukami, K. Fukunaga, N. Takahashi, S. Tamura, Studies on piericidin. *Agric. Biol. Chem.* **34**, 1101–1109 (1970).

44. L. Logie *et al.*, Cellular responses to the metal-binding properties of metformin. *Diabetes* **61**, 1423–1433 (2012).

45. X. Quan *et al.*, The copper binding properties of metformin—QCM-D, XPS and nanobead agglomeration. *Chem. Commun. (Camb.)* **51**, 17313–17316 (2015).

46. P. Repišćák, S. Erhardt, G. Rena, M. J. Paterson, Biomolecular mode of action of metformin in relation to its copper binding properties. *Biochemistry* **53**, 787–795 (2014).

47. I. P. Hargreaves *et al.*, Inhibition of mitochondrial complex IV leads to secondary loss complex II-III activity: Implications for the pathogenesis and treatment of mitochondrial encephalomyopathies. *Mitochondrion* **7**, 284–287 (2007).

48. W. Shen *et al.*, Involvement of a glycerol-3-phosphate dehydrogenase in modulating the NADH/NAD+ ratio provides evidence of a mitochondrial glycerol-3-phosphate shuttle in *Arabidopsis*. *Plant Cell* **18**, 422–441 (2006).

49. R. J. Shaw *et al.*, The kinase LKB1 mediates glucose homeostasis in liver and therapeutic effects of metformin. *Science* **310**, 1642–1646 (2005).

50. G. Zhou *et al.*, Role of AMP-activated protein kinase in mechanism of metformin action. *J. Clin. Invest.* **108**, 1167–1174 (2001).

51. R. W. Hunter *et al.*, Metformin reduces liver glucose production by inhibition of fructose-1-6-bisphosphatase. *Nat. Med.* **24**, 1395–1406 (2018).

52. S. A. Hawley, A. E. Gadalla, G. S. Olsen, D. G. Hardie, The antidiabetic drug metformin activates the AMP-activated protein kinase cascade via an adenine nucleotide-independent mechanism. *Diabetes* **51**, 2420–2425 (2002).

53. Z. Drahota *et al.*, Biguanides inhibit complex I, II and IV of rat liver mitochondria and modify their functional properties. *Physiol. Res.* **63**, 1–11 (2014).

54. S. Larsen *et al.*, Metformin-treated patients with type 2 diabetes have normal mitochondrial complex I respiration. *Diabetologia* **55**, 443–449 (2012).

55. Y. Wang *et al.*, Metformin improves mitochondrial respiratory activity through activation of AMPK. *Cell Rep.* **29**, 1511–1523.e5 (2019).

56. W.-S. Choi, R. D. Palmiter, Z. Xia, Loss of mitochondrial complex I activity potentiates dopamine neuron death induced by microtubule dysfunction in a Parkinson's disease model. *J. Cell Biol.* **192**, 873–882 (2011).

57. Y. Wang, H. Kwon, X. Su, F. E. Wondisford, Glycerol not lactate is the major net carbon source for gluconeogenesis in mice during both short and prolonged fasting. *Mol. Metab.* **31**, 36–44 (2020).

58. J. Xie *et al.*, GPD1 enhances the anticancer effects of metformin by synergistically increasing total cellular glycerol-3-phosphate. *Cancer Res.* **80**, 2150–2162 (2020).

59. P. Cavallo-Perin *et al.*, The hyperlactatemic effect of biguanides: A comparison between phenformin and metformin during a 6-month treatment. *Riv. Eur. Sci. Med. Farmacol.* **11**, 45–49 (1989).

60. M. Tavallaie *et al.*, Moderation of mitochondrial respiration mitigates metabolic syndrome of aging. *Proc. Natl. Acad. Sci. U.S.A.* **117**, 9840–9850 (2020).

61. H. R. Bridges, A. J. Jones, M. N. Pollak, J. Hirst, Effects of metformin and other biguanides on oxidative phosphorylation in mitochondria. *Biochem. J.* **462**, 475–487 (2014).

62. S. Thakur *et al.*, Metformin targets mitochondrial glycerophosphate dehydrogenase to control rate of oxidative phosphorylation and growth of thyroid cancer *in vitro* and *in vivo*. *Clin. Cancer Res.* **24**, 4030–4043 (2018).

63. M. J. MacDonald, I.-U. H. Ansari, M. J. Longacre, S. W. Stoker, Metformin's therapeutic efficacy in the treatment of diabetes does not involve inhibition of mitochondrial glycerol phosphate dehydrogenase. *Diabetes* **70**, 1575–1580 (2021).

64. M. Mochizuki *et al.*, Quantitative reevaluation of the redox active sites of crystalline bovine heart cytochrome *c* oxidase. *J. Biol. Chem.* **274**, 33403–33411 (1999).

65. J. D. Young, D. K. Allen, J. A. Morgan, "Isotopomer measurement techniques in metabolic flux analysis II: Mass spectrometry" in *Plant Metabolism: Methods and Protocols*, G. Sriram, Ed. (Humana Press, Totowa, NJ, 2014), pp. 85–108.

LaMoia et al.
Metformin, phenformin, and galegine inhibit complex IV activity and reduce glycerol-derived gluconeogenesis

PNAS | 9 of 9
https://doi.org/10.1073/pnas.2122287119